Uptake of atmospherically deposited cadmium by leaves of vegetables : Subcellular localization by NanoSIMS and potential risks

Journal of Hazardous Materials

Ouyang, Xiaoxue; Ma, Jie; Zhang, Ran; Li, Pan; Gao, Man et al

https://doi.org/10.1016/j.jhazmat.2022.128624

Journal of Hazardous Materials 431 (2022) 128624

Contents lists available at ScienceDirect

Journal of Hazardous Materials

journal homepage: www.elsevier.com/locate/jhazmat

Research Paper

Uptake of atmospherically deposited cadmium by leaves of vegetables: Subcellular localization by NanoSIMS and potential risks

Xiaoxue Ouyang [a,b], Jie Ma [a,b,*], Ran Zhang [a,b], Pan Li [c], Man Gao [c], Chuanqiang Sun [c], Liping Weng [b,d,*], Yali Chen [a,b], Sun Yan [e], Yongtao Li [f,g]

[a] Key Laboratory for Environmental Factors Control of Agro-Product Quality Safety, Ministry of Agriculture and Rural Affairs, Tianjin 300191, China
[b] Agro-Environmental Protection Institute, Ministry of Agriculture and Rural Affairs, Tianjin 300191, China
[c] School of Earth System Science, Tianjin University, Tianjin 300072, China
[d] Department of Soil Quality, Wageningen University, Wageningen, The Netherlands
[e] Institute of Eco-environmental and Soil Sciences, Guangdong Academy of Sciences, Guangzhou 510642, China
[f] College of Natural Resources and Environment, South China Agricultural University, Guangzhou 510642, China
[g] College of Resource and Environmental Engineering, Jiangxi University of Science and Technology, Ganzhou, Jiangxi 341000, China

HIGHLIGHTS

- Foliar exposure to CdS_N significantly increased Cd concentration in plant tissues.
- Foliar exposure to CdS_N exhibited no phytotoxicity symptoms.
- NanoSIMS revealed Cd detoxification was due to its accumulation in the cell walls.
- Potential health risks related to consuming Cd-exposed vegetable are highlighted.

GRAPHICAL ABSTRACT

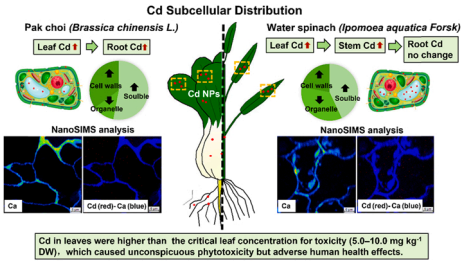

ARTICLE INFO

Editor: Guillaume Echevarria

Keywords:
CdS nanoparticles
Foliar uptake
Phytotoxicity
Subcellular distribution
NanoSIMS
Health risk

ABSTRACT

Atmospherically deposited cadmium (Cd) may accumulate in plants through foliar uptake; however, the foliar uptake, accumulation, and distribution processes of Cd are still under discussion. Atmospherically deposited Cd was simulated using cadmium sulfide (CdS) with various particle sizes and solubility. Water spinach (*Ipomoea aquatica Forsk*, WS) and pak choi (*Brassica chinensis L.*, PC) leaves were treated with suspensions of CdS nanoparticles (CdS_N), which entered the leaves via the stomata. Cd concentrations of WS and PC leaves treated with 125 mg L^{-1} CdS_N reached up to 39.8 and 11.0 mg kg^{-1}, respectively, which are higher than the critical leaf concentration for toxicity. Slight changes were observed in fresh biomass, photosynthetic parameters, lipid peroxidation, and mineral nutrient uptake. Exposure concentration, rather than particle size or solubility, regulated the foliar uptake and accumulation of Cd. Subcellular and the high-resolution secondary ion mass spectrometry (NanoSIMS) results revealed that Cd was majorly stored in the soluble fraction and cell walls, which is an important Cd detoxification mechanism in leaves. The potential health risks associated with consuming CdS-containing vegetables were highlighted. These findings facilitate a better understanding of the fate of atmospheric Cd in plants, which is critical in ensuring food security.

* Corresponding authors at: Agro-Environmental Protection Institute, Ministry of Agriculture and Rural Affairs, Tianjin 300191, China.
E-mail addresses: majie@cass.cn (J. Ma), wengliping@caas.cn (L. Weng).

https://doi.org/10.1016/j.jhazmat.2022.128624
Received 9 November 2021; Received in revised form 16 February 2022; Accepted 1 March 2022
Available online 4 March 2022

1. Introduction

Cadmium (Cd) is a well-known toxic element and an environmental pollutant. Most anthropogenic Cd is first emitted into the atmosphere, and then precipitates onto soil and water (Shao et al., 2013). Several recent studies have revealed the importance of atmospheric deposition as a source of Cd in agro-ecosystems (Luo et al., 2009; Pontevedra-Pombal et al., 2013; Shao et al., 2013). Prolonged Cd exposure not only reduces crop yield and food quality (Rizwan et al., 2017), but also threatens human health by its possible transfer to humans via the food chain (Kubier et al., 2019).

Anthropogenic Cd emission into the atmosphere mainly results from fossil fuel combustion, non-ferrous metal smelting, iron and steel smelting, municipal solid waste incineration, cement and phosphorus fertilizer production (Shao et al., 2013). The major Cd species typically emitted are oxides, sulfides, chlorides, and elemental Cd (Hassanien and Shahawy, 2011). After emission, Cd tends to be preferentially associated with small-sized particles (< 1 μm) with long residence times in the atmosphere (Louie et al., 2005; Canepari et al., 2008), and can be transported over long distances (Zereini et al., 2005; Shahid et al., 2017), subsequently accumulating in soil, water, and vegetation via wet or dry deposition. Deposited Cd mainly present as the water-soluble and exchangeable fractions, is highly mobile and bioavailable (Fernandez-Olmo et al., 2014; Lee et al., 2015). These fractions are potentially activated at low pH and slightly reduced conditions, which release Cd into the environment (Lee et al., 2015). Furthermore, cadmium sulfide (CdS) is an important component emitted during non-ferrous metal production and coal combustion (Dillner et al., 2005; Kuloglu and Tuncel, 2005). The engineered nanoparticles used in many sectors, including fluorescence imaging, biosensing, and green-synthesized nano-pesticides, are responsible for increasing the level of CdS nanoparticles released into the environment in recent decades (Wang et al., 2012; Bu et al., 2013).

Plants absorb trace metals from the atmosphere via soil-root transportation and atmospheric foliar absorption (Schreck et al., 2014; Kumar et al., 2019). Traditionally, most studies have reported Cd uptake by roots (Verma et al., 2007; Wu et al., 2018; Shi et al., 2019); however, in recent years, foliar uptake of Cd has received more attention. Previous studies have identified the direct relationship between trace metal concentrations in plant leaves and atmospheric deposition (De Temmerman et al., 2012; Feng et al., 2019; Cao et al., 2020). For example, atmospheric depositions contribute to 20–85% of shoot Cu and Cd in areas near a copper smelter (Liu et al., 2019). The potential phytotoxicity and health risks associated with consuming plants exposed to Cd ions (Cakmak et al., 2000a, 2000b; Cakmak et al., 2000a, 2000b; Harris and Taylor, 2001) by foliar spraying has also been reported previously. For example, wheat biomass and grain yield are affected by foliar application of $CdCl_2$ solution, which significantly increases Cd concentrations in wheat tissues (Li et al., 2020a, 2020b). However, particulate Cd released from technological processes into the atmosphere has received limited attention to date (Vecerova et al., 2016; Vecerova et al., 2019). The major focus of research in this area has been on the effect of atmospheric Cd nanoparticles on plant metabolism and phytotoxicity; whereas less attention has been directed toward the uptake, translocation, and distribution mechanisms of Cd nanoparticles.

Previous studies have revealed that particles and chemical elements enter the leaves via the stomata or the cuticle (Schönherr and Luber, 2001; Schonherr, 2006; Eichert and Goldbach, 2008; Eichert et al., 2008). Furthermore, nanoparticles (such as Ag, TiO_2, and CeO_2) on plant surfaces can reportedly penetrate the leaves and transfer to other tissues (Hong et al., 2014; Larue et al., 2014a, 2014b). However, the distribution and translocation of atmospheric Cd nanoparticles in plants entering via the stomata and cuticle are unclear. In addition, studies have shown that the subcellular distribution of Cd is involved in plant tolerance and detoxification (Wu et al., 2005; Fu et al., 2011). A previous study found that approximately 60% of Cd was localized in the cell wall fraction of lettuce (Ramos et al., 2002). In Cd-resistant barley genotypes, Cd has been observed to be integrated mostly with pectates and proteins in the soluble and cell wall-containing fractions (Wu et al., 2005). Previous studies have identified the precise chemical, biological, and physical mechanisms of trace metals on bio-uptake at the cellular level (Lead and Wilkinson, 2006a, 2006b; Lead and Wilkinson, 2006a, 2006b; Worms et al., 2006). However, current knowledge regarding the subcellular distribution of Cd is mainly associated with the root absorption pathway instead of the foliar pathway.

Therefore, in our study, the Cd uptake, accumulation, and distribution in plants exposed to CdS nanoparticles (CdS_N) through the leaves were examined, and phytotoxicity and human health impacts were assessed by foliarly treating water spinach (*Ipomoea aquatica Forsk*, WS) and pak choi (*Brassica chinensis L.*, PC) with aqueous suspension of CdS_N and CdS bulk particles (CdS_B) to compare the effects of particle size and solubility. Meanwhile, the cellular and subcellular distribution of Cd in leaves was mapped via the combined use of subcellular analysis and the high-resolution secondary ion mass spectrometry (NanoSIMS) (NanoSIMS 50,Cameca). This newly generated information aids in understanding the behavior and ultimate fate of atmospheric Cd in plants, and the potential risk of Cd transfer via food chains.

2. Materials and methods

2.1. Experimental material preparation and characterization

Pristine CdS_N (98% purity) was purchased from Shanghai Xingzi New Material Technology Development Co., Ltd, China. The shape and nominal diameter of CdS_N were characterized by scanning electron microscopy (SEM) (OxfordX-MAX, Zeiss) and an atomic force microscope (AFM) (Bruker Dimension ICON, Bruker), respectively. CdS_B (98% purity) was purchased from Shanghai Macklin Biochemical Co., Ltd, China. The hydrodynamic diameter and zeta potential of the CdS_N, and zeta potential of the CdS_B suspension were measured by dynamic light scattering (DLS) using a NanoZS (Zetasizer Nano ZS, Malvern). The hydrodynamic diameter of the CdS_B suspension was measured by a laser diffraction particle size analyzer (Malvern Zetasizer 3000, Malvern). In addition, the dissolution kinetics of CdS_N and CdS_B (125 mgL^{-1}) in ultrapure water were investigated at different time intervals (1 −48 h). The CdS_N and CdS_B suspensions were centrifuged twice at 10,000 rpm for 30 min and strained through a filter membrane (0.1 μm) to separate CdS_N and CdS_B from the suspension. The dissolved Cd^{2+} ion concentrations were determined using inductively coupled plasma mass spectrometry (ICP-MS) (Elan DRC-e, PerkinElmer).

CdS_N was mainly sheet-shaped with a nominal diameter of 130 ± 25 nm and a thickness of 15 ± 8 nm (Fig. S1). CdS_N suspended in ultrapure water was agglomerated with a hydrodynamic diameter of 278.6 ± 40 nm (Fig. S2a). Individual CdS_B were approximately 2.19 − 45.70 μm (average 7.78 μm) in hydrodynamic diameter (Fig. S2b). The average dissolution rates of Cd^{2+} ions released from the CdS_N and CdS_B suspensions were ~40.0% and 0.4%, respectively (Fig. S3). The concentrations of ionic Cd species resulting from CdS_N dissolution were comparable with those of a previous study that discusses the effect of $CdCl_2$ solution on wheat (Li et al., 2020a, 2020b). At 48 h, the particle size of CdS_N was 301.8 ± 131.2 nm (Fig. S4), whereas CdS_B remained precipitated in the solution. The properties of the particles, and SEM and AFM images are shown in SI1.

2.2. Plant culture and exposure

The widely cultivated WS and PC have short life cycles; WS has thin, hollow stems with long, flat, arrowhead-shaped leaves, whereas PC has larger leaves with a smooth surface and no evident stem. Moreover, WS and PC can accumulate higher amounts of Cd when grown in Cd-contaminated soil (Yang et al., 2009; Yang et al., 2010). For the exposed experiment, six young plantlets (4 or 5 leaves per plant with an area of 3

−6 cm^2 per leaf) were grown per pot in nutrient soil in a glasshouse for 3 weeks. Seedling-raising details, the physicochemical properties of the nutrient soil, and cultivation conditions are provided in SI 2.

CdS_N at different concentrations (0 [control, CK], 2.5, 25, and 125 mg L^{-1}) and CdS_B (125 mg L^{-1}) suspensions prepared in ultrapure water were sonicated (100 W, 40 kHz) for 30 min in a water bath. Thereafter, 2 mL CdS was applied to the entire plant leaves using a dropper, while ensuring that no liquid dropped from the surface, until a layer of droplets was visible on all leaves. This procedure was performed twice, with the applications spaced 5 days apart. Plants were harvested 5 days after the last foliar exposure. Based on our atmospheric monitoring data for an agricultural site in Tianjin, China, the Cd concentrations in $PM_{2.5}$ and PM_{10} are 125 and 150 mg kg^{-1}, respectively (unpublished data); The simulated CdS deposits in this study were prepared with concentrations of 0, 2.5, 25, and 125 mg L^{-1}. The final Cd amounts deposited were 0, 1.3, 13.0, and 64.8 μg per plant for the 0, 2.5, 25, and 125 mg L^{-1} CdS concentrations, respectively, which corresponded to a quantity of Cd per area of 0, ~10.4, ~104.0, and ~518.4 ng cm^{-2} of leaf surface for PC, and 0, ~16.9, ~169.0, and ~841.6 ng cm^{-2} of leaf surface for WS, respectively. These values ranged between potential aerial deposition and extreme Cd pollution concentrations (Schreck et al., 2012; Pan and Wang, 2015). During the exposure period of 10 days, the soil surface was covered with plastic film to prevent contamination. All pot treatments were conducted in triplicate.

The harvested plants were divided into the roots, stems, and leaves. To remove excess Cd, plants were thoroughly rinsed with tap water, immersed in 0.01 M $CaCl_2$ for 20 min, washed thrice with deionized water and ultrapure water, and then gently wiped with a tissue (Hong et al., 2014). The fresh biomass was determined, and the plants were subsequently pooled and prepared according to the experimental procedures detailed below (Sections 2.3–2.5). The effect of CdS accumulation on leaf surfaces was evaluated by visualizing the unwashed leaf surfaces using SEM-EDS to determine leaf surface element speciation, either on the spots of interest or in the scanning mode, as described in SI 3.

2.3. Phytotoxicity tests

Before harvest, relative chlorophyll content and photosynthetic index were measured using a SPAD-502 chlorophyll meter (SPAD, Minolta Camera) and a portable infrared gas analyzer (LI-COR 6400 XT, LI-COR), respectively. The stomatal parameters were determined using optical microscopy (CX31RTSF, Olympus). After harvesting, fresh leaves were subjected to enzymatic activity assays and lipid peroxidation detection using kits purchased from Geruisi Biotechnology Co., Ltd, China according to the manufacturer's instructions. Superoxide dismutase (SOD, EC 1.15.1.1) and catalase (CAT; EC 1.11.1.6) activities were determined using total superoxide dismutase assay and CAT assay kits, respectively. Lipid peroxidation was determined using the thiobarbituric acid method. Malondialdehyde (MDA) levels were determined using malondialdehyde kits. A complete description is available in SI 4.

2.4. Accumulation of trace metals and subcellular distribution of Cd in plant tissues

Fresh plants were oven-dried at 75 ℃ for approximately 48 h and subsequently were weighed, powdered, and passed through a 0.45-mm sieve. The dried samples were then digested with HNO_3-$HClO_4$ (5:1, v/v). Concentrations of Cd and other elements in the plant matter (P, Ca, Mg, K, Fe, Zn, Cu, and Pb) were determined using ICP-MS. Fresh plants were subjected to subcellular analysis using a previously described method (Fu et al., 2011; Xin and Huang, 2014) with some modifications. Cd concentrations in the cell walls, organelles, and the soluble fraction were quantified using ICP-MS. A certified reference plant material [GBW 07603(GSV-2)] was included for quality control. The recoveries ranged from 88.9% to 102.6%, which were obtained using the method described in SI 5.

Moreover, Cd adsorption rate, Cd concentrations in plant tissues, and Cd translocation factors (TFs) were calculated. A complete method description of the methods and the formulas for these calculations are provided in SI 6–8.

2.5. NanoSIMS analysis of leaf samples and health assessment upon consumption

NanoSIMS is a sensitive in situmapping technique capable of locating and quantifing ultra-trace elemental distributions in biological samples at high resolution (50 nm to few microns) (Kilburn and Clode, 2014). In this study, cellular and subcellular elemental distributions in leaves were mapped using NanoSIMS. Sampling and sample preparation were performed using a previously described method (Tartivel et al., 2012; Kilburn and Clode, 2014) with some modifications. Contaminated leaf samples of approximately 2 × 2 mm in size were rapidly transferred into centrifuge tubes containing 2.5% glutaraldehyde and fixed for 3 days. It was dehydrated using a gradient of water-anhydrous ethanol and then gradually infiltrated with Spurr resin. Thereafter, the resin blocks were trimmed to a thickness of 1 μm using an ultra-microtome and finally coated with a 5 nm conductive layer of Pt coating metal. Leaf sections were examined separately using Cs^+ and O^- primary ion beams. A complete description is available in SI 9.

In addition, the human health impact of consuming CdS-containing vegetables was assessed by calculating the daily pollutant intake (EDI, μg kg^{-1} day^{-1}), non-carcinogenic risk index (HQ), and maximal acceptable daily intake of the contaminated plant material (MDI, μg kg^{-1} day^{-1}). The complete calculation is provided in SI 10.

2.6. Statistical analysis

Statistical analyses and the figures were performed using the R software version 4.0.3. Datasets were tested for normality and homoscedasticity using the Shapiro-Wilk and Bartlett's test, respectively. An analysis of variance (ANOVA) and a subsequent Tukey's HSD test was performed at a statistical significance level of $p < 0.05$.

3. Results and discussion

3.1. CdS uptake and accumulation

The Cd concentrations in WS and PC were measured after exposure to CdS_N and CdS_B, as shown in Fig. 1. In CK, the Cd concentrations in the roots, stems, and leaves of the two plants were low, ranging from 0.16 to 0.52 mg kg^{-1} (Fig. 1). Except for WS roots, other tissues of WS and the whole plant of PC observed an increase in Cd concentrations compared to those in CK (Fig. 1). Cd concentrations in WS and PC leaves significantly increased at 125 mg L^{-1} CdS_N, up to 39.8 and 11.0 mg kg^{-1}, which were 100 and 36 times higher than those in CK, respectively (Fig. 1a and d); meanwhile, Cd concentrations in WS stems and PC roots were 4.5 and 2.2 times higher than those in CK, respectively (Fig. 1b and e). The results reveal the possibility that CdS_N penetrates the leaf surface and is transferred to other plant tissues. Approximately 5–13% of the total exposed foliar Cd was absorbed by the plants (Table S2), which elevated plant Cd concentration ($[Cd]_{plant}$), resulting in a $[Cd]_{plant}$ of up to 0.3–15.7 and 0.3–6.4 mg kg^{-1} in WS and PC, respectively (Table S4). The $[Cd]_{plant}$ and $[Cd]_{leaves}$ in WS and PC were positively correlated with the applied Cd concentrations (Table S5). Moreover, Cd concentrations in different plant tissues decreased in the following the order: leaves > stems > roots, with TFs ranging from 0.01 to 0.32 (Tables.S3 and S4). In a previous study on lettuce contaminated with Pb and Cd, the TFs were 0.06 and 0.28, respectively, after 6 weeks of foliar metal exposure (Xiong et al., 2014), suggesting that CdS_N penetrated the leaf surface, but their translocation through the leaf tissue was limited. Similar TFs

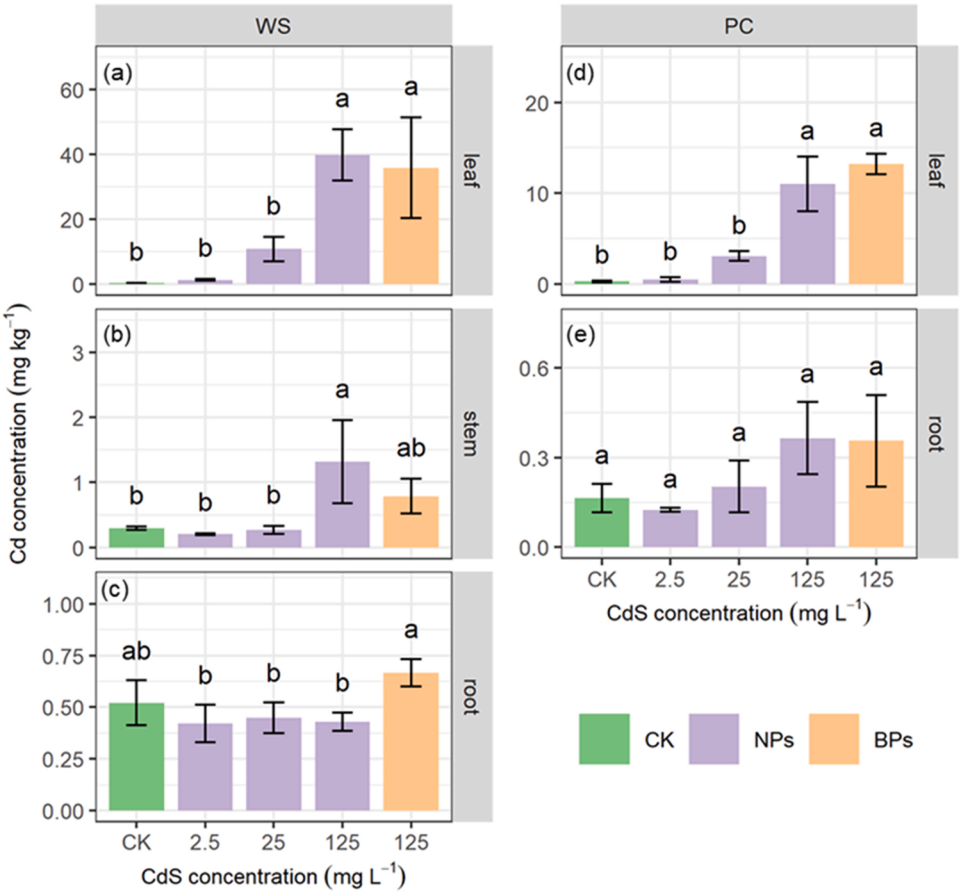

Fig. 1. Cadmium (Cd) concentrations in (a) the leaves, (b) stems, and (c) roots of water spinach (*Ipomoea aquatica Forsk*, WS), and (d) the leaves and (e) roots of pak choi (*Brassica chinensis L.*, PC) after foliar cadmium sulfide (CdS) nanoparticle (CdS_N)/CdS bulk particle (CdS_B) (0, 2.5, 25, and 125 mg L^{-1}/125 mg L^{-1}) exposure. The values are calculated as mean ± standard deviation (SD). Different letters (a, b, c) indicate that values significantly differ in the same vegetable under different Cd concentrations ($p < 0.05$).

were previously observed via the foliar pathway for lettuce and cabbage contaminated with CuO nanoparticles (TF ranged from 0.04 to 0.33) (Xiong et al., 2017). The lower TFs in the present study may be attributed to shorter exposure times and the particular plant species studied, and indicate that among the excess Cd accumulated in plant leaves, a portion was translocated to the stems or roots (Harris and Taylor, 2001; Xiong et al., 2014).

Under foliar Cd transfer, a four-fold higher Cd concentration was observed in WS leaves than that in PC leaves (Fig. 1a and d), which was attributed to species variation and a relatively higher biomass of PC leaves (Fig. S9a and e). Furthermore, CdS_B exposure significantly increased the Cd concentrations in the plants of both species; however, under similar concentrations of CdS_B and CdS_N, the Cd accumulated in WS and PC did not prominently differ. The high solubility of CdS_N used in this study suggests that the ionic Cd species resulting from the dissolution of CdS_N contributed to foliar transfer to a limited extent. In other words, both the highly soluble CdS_N and the less soluble CdS_B entered plant leaf tissues. This indicates that the particle size and CdS solubility parameters considered in this study did not considerably impact Cd accumulation in our test plants. Therefore, the exposed Cd concentration may be the main factor controlling Cd accumulation in these species.

After CdS_N (125 mg L^{-1}) exposure, most CdS_N were deposited as micrometric aggregates on WS and PC leaf surfaces, either around the stomata or even inside the stomata (Fig. S5a and b). Although CdS_N particles were faintly visible inside the stomata, Cd visible inside and around the stomata was identified using EDS (Fig. 2a–d), indicating the entry of CdS_N into the stomata was through the stomata chamber. Furthermore, an area from the leaf cross-sections was selected for analysis using EDS, and the corresponding EDS spectrum showed the presence of Cd inside the leaf (Fig. 2e and f). A previous study found $PM_{2.5}$-Pb enrichment in the stomata of Chinese cabbage (Gao et al., 2021). Previous studies have reportedly observed some nanoparticles in the leaf cuticular waxes and the stomatal chamber of the leaf surface after foliar nanoparticle exposure (Uzu et al., 2010; Schreck et al., 2012; Larue et al., 2014a, 2014b); however, in this study, CdS_N entrapped in the leaf cuticle and/or in the cuticular waxes was not observed using SEM. In addition, CdS_B was enriched on the foliar surfaces and across sections of WS and PC leaves (Fig. S6). The stomatal width and length on the WS adaxial epidermis were 9.26–19.22 and 18.16–37.3 μm, respectively, and those on the PC adaxial epidermis were 5.99–1.76 and 10.17–20.00 μm, respectively (Table S7). Both individual CdS_N and most of their aggregates in ultrapure water were sufficiently sized to facilitate their entry through the stomata, along with a few CdS_B, which is supported by the results of SEM-EDS and stomatal data. In addition to the stomatal pathway, the cuticular pathway is an alternative route for nanoparticle entry (Schreck et al., 2012). In general, metals can penetrate the cuticle via two pathways: the lipophilic pathway and the hydrophilic pathway (Schreiber and Önherr, 2009). However, these two cuticle pathways of cuticle penetration are mainly described for fine particles (i.e., those of a few nm in diameter) (Fernández and Eichert, 2009). The slightly larger diameter of the individual CdS_N/CdS_B and their aggregates hinders their direct uptake via the cuticle pore (~2 nm diameter) (Uzu et al., 2011). In addition, internalization of CdS_N/CdS_B within the epicuticular wax was not observed in the SEM images. Hence, stomatal openings were likely the main Cd uptake pathways in the leaves of the two species. This is consistent with the previous results (Larue et al., 2014a, 2014b; Xiong et al., 2017).

3.2. CdS phytotoxicity

The effects of CdS_N and CdS_B on WS and PC were assessed based on

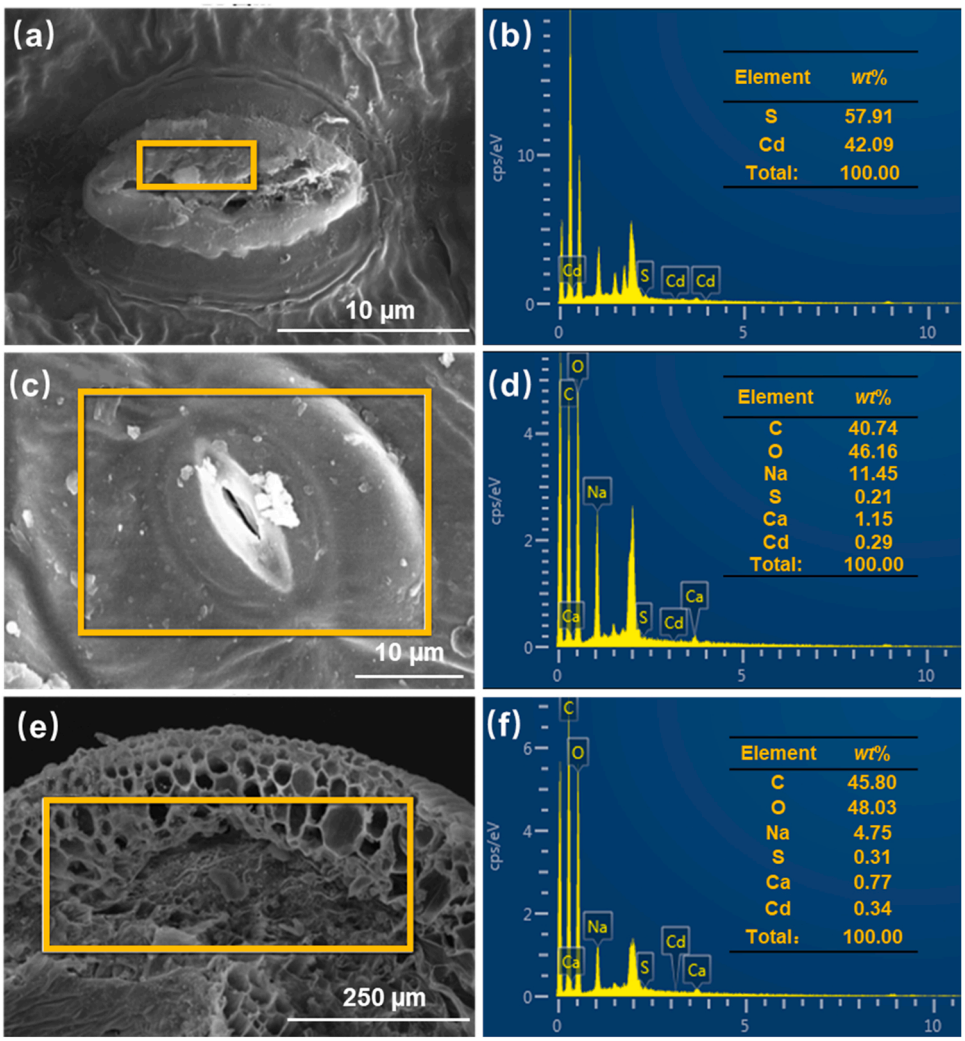

Fig. 2. Scanning electron microscopy (SEM) images of the stomata of (a) pak choi (*Brassica chinensis L.*, PC) and (c) water spinach (*Ipomoea aquatica Forsk*, WS) and corresponding energy dispersive X-ray spectroscopy analysis (b and d) after foliar cadmium sulfide (CdS) nanoparticle (CdS_N) exposure (125 mg L^{-1}). SEM image of (e) cross-sections of WS and (f) the corresponding EDS analysis.

plant biomass, chlorophyll content, photosynthetic parameters, antioxidant enzymatic activity, lipid peroxidation, and accumulation of other elements. Foliar Cd application affected the MDA activity of PC leaves, which increased by 51–73% more than that in the CK(Fig. 3i). SOD and CAT activities of PC leaves increased with no noticeable difference (Fig. 3g and h). For WS, the total activities of SOD and MDA in the leaves and stems were higher than those of the CK, with no changes observed, while the irregularly observed CAT activity was unclear (Fig. 3a–f). MDA generated during lipid peroxidation serves as an indicator of cell membrane injury. The increased MDA levels in the leaves of the two species suggest that foliar CdS_N exposure induced oxidative damage, especially in PC. The increase in SOD and CAT activity suggests that when CdS_N are in contact with leaves, they can modify the enzyme activity of both species. However, the effect observed was limited in this study.

The fresh weight of the roots, stems, leaves, and the total biomass remained unchanged compared to that of the CK regardless of the treatment concentration (Fig. S9). Similarly, the chlorophyll contents in the two species presented no noticeable changes (Fig. S10). The net photosynthesis (Pn) of WS significantly decreased by 38% compared to that of the CK at high CdS_N concentration, but no changes were observed in the other photosynthetic parameters of WS and all of the photosynthetic parameters of PC (Fig. S11a–h). The reduction in the leaf photosynthetic rate under metal stress can inhibit plant growth (Rodriguez-Serrano et al., 2009); however, in this study, plant growth was unaffected by the photosynthetic rate. Additionally, foliar CdS_N application did not significantly affect the accumulation of other metals (Table.S8), which indicates that other metal concentrations in WS and PC shoots could be maintained at a certain level under foliar CdS_N application. Furthermore, no significant difference in the above parameters was observed between CdS_N and CdS_B treatments under similar Cd levels. This indicates that the Cd particle size and solubility considered in this study do not significantly impact the phytotoxic parameters.

Generally, excessive Cd may cause leaf chlorosis, inhibition of photosynthesis, growth retardation, lipid peroxidation, root browning, reduced biomass, and even death in most plants (Chang et al., 2013; Rizwan et al., 2016a, 2016b). Cd concentration in leaves higher than the critical leaf concentration for toxicity (5.0–10.0 mg kg^{-1} DW), was toxic to most plants, causing more than a 10% decrease in yield (White and Brown, 2010). For example, Cd exposure (10 μM Cd) in tomato plants not only increased the Cd concentration in leaves (184 ± 54 mg kg^{-1} dry weight [DW]), but also reduced tomato growth and caused and leaf chlorosis and necrosis (Lopez-Millan et al., 2009). However, in the present study, noticeable toxic symptoms were not observed in plants regardless of Cd treatment, despite the Cd concentrations in leaves (WS for 39.8 and PC for 11.0 mg kg^{-1} DW) in the 125 mg kg^{-1} treatments being greater than the critical concentration of toxicity. This may be attributed to Cd uptake pathways; the metal toxicity varies with the

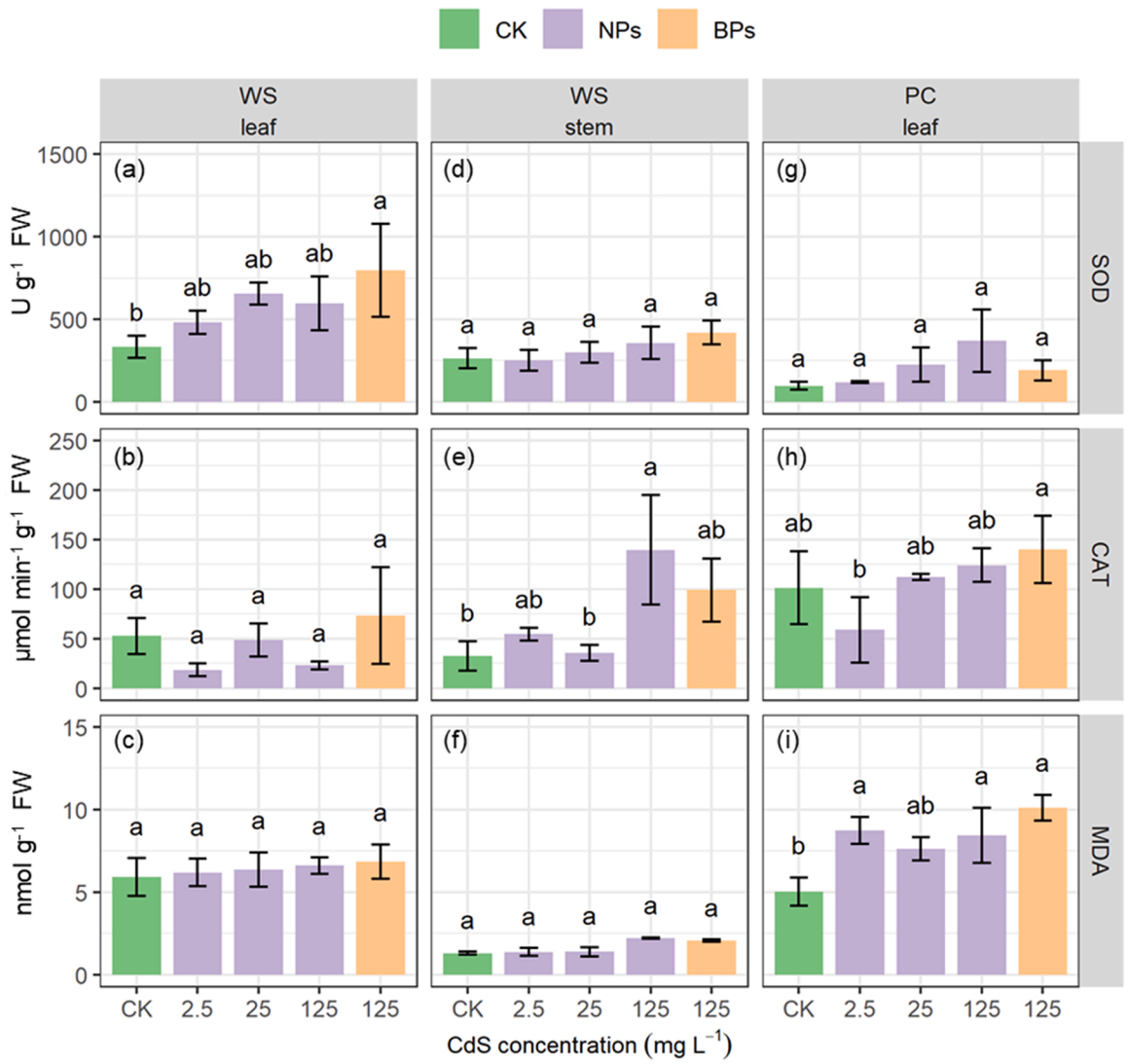

Fig. 3. Superoxide dismutase (SOD), catalase (CAT), and malondialdehyde (MDA) levels in the leaves and stems of water spinach (*Ipomoea aquatica Forsk*, WS, a–c and d–f) and the leaves of pak choi (*Brassica chinensis L.*, PC, g–i) after foliar cadmium sulfide (CdS) nanoparticle (CdS_N)/CdS bulk particle (CdS_B) (0, 2.5, 25 and 125 mg L^{-1}/125 mg L^{-1}) exposure. The values were given as mean ± SD (standard deviation). Different letters (a, b, c) indicated values significantly different in the same vegetable under the different Cd concentrations ($p < 0.05$).

mode of entry in plants, that is, whether it occurs via roots or foliage (Shahid et al., 2017). Cu supplementation via the roots or leaves showed different effects on soybean plants, and the decrease in plant biomass and inhibition of root growth were more pronounced under root exposure compared to that of foliar exposure (Bernal et al., 2007). This indicates that foliar Cd exposure may decrease plant toxicity more than that during root Cd exposure. Hence, the detoxification mechanism of Cd via leaf absorption necessitates further study.

3.3. Distribution of Cd in subcellular fraction of plants

Subcellular distribution of metals in plants represents the internal tolerance and detoxification mechanisms of the species (Zhang et al., 2015). The results regarding the subcellular distribution of Cd in WS leaves and stems and PC leaves after foliar CdS_N application are shown in Table S9 and Fig. 4. Overall, Cd supplementation increased Cd concentrations in different subcellular fractions of WS and PC leaf tissues. In both WS and PC leaves, most Cd was present in the soluble and cell wall fractions, while a minor portion was associated with the organelle. Compared to the CK, Cd concentrations in the cell wall, organelle, and soluble fractions increased by 3.2–516.8-, 4.9–40.7-, 4.7–106.0-folds and 1.5–37.1-, 1.7–36.4-, 1.3–20.5-folds in the leaves of WS and PC, respectively (Table S9). Cd concentrations displayed no considerable differences among the subcellular fractions of WS stems.

Cd presented a distinct distribution pattern in WS and PC leaf tissues. In WS leaves, the cell wall, soluble and organelle fractions of retained Cd accounted for 14.9–60.9%, 27.7–54.8%, and 11.4–40.0%, respectively (Fig. 4a). In PC leaves, the intracellular Cd stored in the cell wall, soluble, and organelle fractions accounted for 30.8–43.7%, 33.9–47.9%, and 17.9–23.2%, respectively (Fig. 4c). As the concentration increased to 125 mg L^{-1}, the proportion of Cd stored in the cell wall increased, whereas that in the organelle and the soluble fractions decreased. The results indicate that Cd was trapped and gradually accumulated in the cell wall as the Cd concentration increased. Previous root studies have demonstrated that the cell walls act as the key site for preferential Cd binding in ramie (Zhu et al., 2013) and lettuce (Ramos et al., 2002; Zornoza et al., 2002). Cell wall surfaces, mainly composed of polyose (including cellulose, semi-cellulose, and lignin, etc.) and protein, are negatively charged, and thus can bind and restrict the transportation of Cd ions across the cytomembrane (Fu et al., 2011). Additionally, the cell and vacuole sap have several organo-ligands (mainly sulfur-rich peptides and organic acids), which can complex with Cd, resulting in

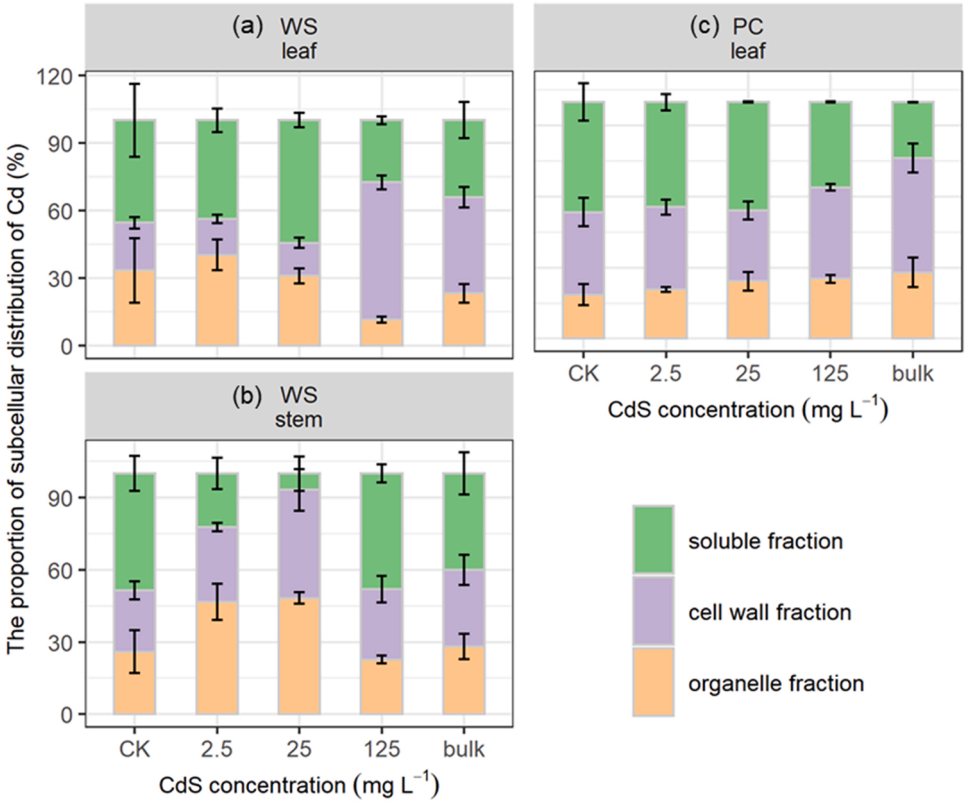

Fig. 4. Subcellular distribution ratio of cadmium (Cd) in (a) the leaf and (b) the stem tissues of water spinach (*Ipomoea aquatica Forsk*, WS) and (c) the leaf tissues of pak choi (*Brassica chinensis L.*, PC) after foliar cadmium sulfide (CdS) nanoparticle (CdS_N)/CdS bulk particle (CdS_B) (0, 2.5, 25, and 125 mg L^{-1}/ 125 mg L^{-1}) exposure.

decreased free ion activity and immobilized Cd in the soluble fraction (Pittman, 2005; Fu et al., 2016). Furthermore, Ag nanoparticles reportedly accumulated less Ag in sensitive tissues/organelles via foliar exposure, resulting in less deleterious effects than root exposure (Li et al., 2020a, 2020b). In this study, Cd was mostly observed in the cell wall and soluble fractions, and a minor portion was present in the organelle fraction, which may be an effective detoxification mechanism for Cd leaf absorption.

Furthermore, in WS stems, Cd in the soluble fraction ranged from 7.1% to 48.1%, while Cd in the cell wall fraction accounted for 24.9–44.5% (Fig. 4b). Although most Cd in the CK was present in the soluble fraction in WS leaves and stems, the proportion of Cd at different exposure levels in different subcellular fractions was inconsistent. This was seemingly associated with the different response mechanisms to Cd stress by different plant organs. In addition, the proportions of Cd in the organelle fraction differed between the two species (Cd proportion in organelles: WS > PC), suggesting that Cd was readily distributed into the organelle fractions of WS. Hence, Cd may affect the normal function of organelles, which consecutively induces plant physiological disorders, thereby causing Cd toxicity. However, WS had no evident toxic symptoms caused by Cd (Figs. S9–11), which may be attributed to the varied levels of Cd tolerance in different plants, which display specific characteristics during metal uptake, translocation, and compartmentalization (Hao et al., 2015). Moreover, no evident difference was observed in Cd subcellular distribution in WS and PC between CdS_N and CdS_B at similar concentrations. This indicates that the particle size and solubility of Cd considered in this study do not significantly affect the subcellular distribution of Cd in the experimental plants.

3.4. Micro-distribution of elements in cells

The infected leaves of WS and PC after foliar CdS_N (125 mg L^{-1}) exposure were observed using NanoSIMS. A primary Cs^+ ion beam was scanned across the surface of the sections, and the sputtered secondary ions were extracted using a double-focusing mass spectrometer to ensure the acquisition of secondary negative ion elemental maps of interest. Subsequently, the same areas were examined using a O^-primary ion beam to map the positive ion elemental maps.

A $^{12}C^{14}N^-$ ion image generated to illustrate the morphology of organic materials (Smart et al., 2007; Smart et al., 2010) reveals that the cell morphology of WS and PC leaves were well-preserved (Fig. 5a and f). The $^{40}Ca^+$,$^{23}Na^+$,$^{28}Si^+$,$^{56}Fe^+$, and $^{16}O^-$ maps further confirmed the outline of the leaf cellular structures of WS and PC (Fig. 5c and h, Fig. S12a-c,e,f-h,j), similar to the $^{12}C^{14}N^-$ image. $^{32}S^-$ ion images indicated that there was sulfur (S) enrichment in the cell walls (Fig. 5b and g). S is a critical nutrient for plant growth and development. Soluble anionic sulfate, which is the primary S form for plant adsorption and utilization, can be directly absorbed by the plant roots via sulfate transporters located on the cell membrane (Mugford et al., 2011). The findings of the present study indicate that, along with root adsorption, the stomatal openings may be another important S uptake pathway in plants, similar to that of Cd.

Generally, zinc (Zn) and Cd generated substantially low secondary ion yields after bombardment with the O^- beam (Ondrasek et al., 2019). Thus, although NanoSIMS requires higher Zn and Cd concentrations compared with other elements, clear Zn and Cd signals can be obtained from biological specimens using this technique. In this study, the Zn and Cd signals were weaker than those of the other elements. The $^{64}Zn^+$ ion was distributed in all cell fractions and enriched in the cell walls of WS and PC (Fig. S12d and i). Zn can be readily transported from the roots to the shoots (e.g., photosynthesizing leaves) via xylem, and then gradually redistributed to the growing plant parts via phloem (Page and Feller, 2005; Riesen and Feller, 2005). Cd and Zn share the same transmembrane transporter and binding compounds in plants owing to their

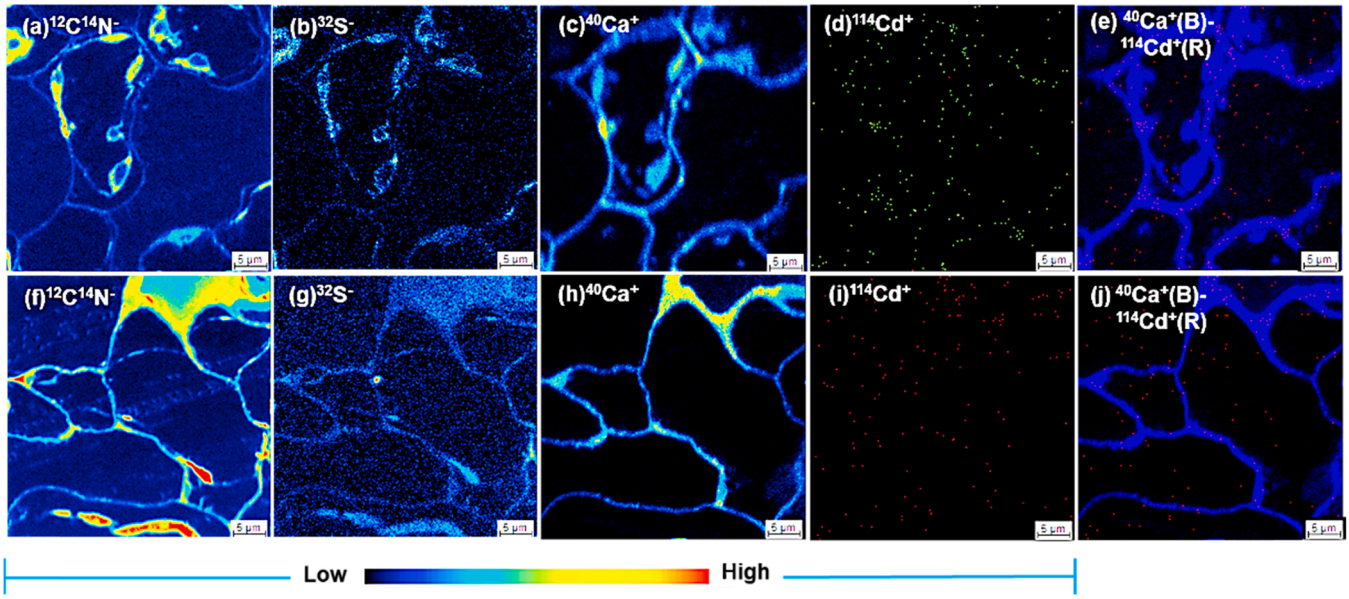

Fig. 5. NanoSIMS elemental maps (50 μm × 50 μm) of (a)–(d) water spinach (*Ipomoea aquatica Forsk*, WS) and (f)–(i) pak choi (*Brassica chinensis L.*, PC) leaf tissues after foliar cadmium sulfide (CdS) nanoparticle (CdS_N) exposure at 125 mg L^{-1} obtained using both beam polarities: Cs^+ to map $^{12}C^{14}N^-$ and $^{32}S^-$, and O^- to map $^{40}Ca^+$, $^{114}Cd^+$. (e) and (j) show the composite (dual) elemental maps of WS and PC, respectively, showing the relative locations of Cd (red) and calcium (Ca; blue).

similar chemical properties (Clemens and Ma, 2016; Qaswar et al., 2017). Hence, Cd may be absorbed by leaves via Zn transporters. This may explain why the $^{114}Cd^+$ ion image showed a similar pattern to that of $^{64}Zn^+$ (Fig. S12k and l). The $^{114}Cd^+$ and composite ($^{114}Cd^+$ and $^{40}Ca^+$) images showed that it is distributed in all cell fractions (Fig. 5d, e, i, and j). Moreover, Cd signal indices in the subcellular fractions of the two species showed that the majority of the Cd signals were detected in the cell walls of both WS and PC, which were 64.8% and 46.8% of the total signals, respectively (Table S10). These results are consistent with the subcellular data, confirming Cd enrichment in cell walls, where the proportion of Cd stored in the cell walls of both WS and PC was 60.9% and 43.6%, respectively (Fig. 4). The Cd signal densities were 0.47 and 0.23, and Cd intensity per unit area was 83.15 and 19.60 in the cell walls of WS and PC, respectively, which are considerably higher than the Cd signal density (0.06 and 0.05, respectively), and Cd intensity per unit area (9.78 and 4.77, respectively) of the other fractions (Table S10). This indicates that Cd was mainly accumulated in the cell walls of WS and PC plants treated with 125 mg L^{-1}. Similarly, using NanoSIMS mapping, accumulation in the various root apical tissues of radish exposed to short-term Cd in situ confirmed the epidermal root cells as preferential sites of Cd uptake (Zhou et al., 2017). Compared to traditional subcellular analysis, NanoSIMS analysis is more direct and can be precisely targeted to investigate Cd distribution at higher resolution. Thus, combining NanoSIMS with subcellular analysis for quantification, localization, and visualization can provide important clues regarding Cd transportation and storage in plant cells.

Cd entering the intercellular gas space of leaves via the stomata is deposited on the cell walls of the substomatal cavity or neighboring cells (Dietz and Herth, 2011). Then, Cd partly enters the intercellular space and associates with the outer apoplast, partly traverses the cell wall and enters the symplast (Dietz and Herth, 2011; Li et al., 2020a, 2020b). When Cd is transported into the symplast from the leaf surface, a portion of it is transported into the phloem, and the rest might be sequestrated in the non-labile subcellular compartments of leaf tissues (Tavarez et al., 2015; Li et al., 2020a, 2020b). The negatively-charged cell wall structures may bind with Cd ions (Wang et al., 2008), which is the first barrier protecting the protoplasts from Cd ion toxicity (Ramos et al., 2002; Xu et al., 2012). However, a cell's capacity to compartmentalize Cd within the cell wall usually has limitations (Fu et al., 2011). Once the cell wall binding sites reach the saturation point, some Cd enters the cell and vacuoles via the cytomembrane, and is then stored in the soluble fraction (mainly in vacuoles) (Rodriguez-Rosales et al., 2008; Wang et al., 2015). The Cd maps and signals generated in the present study show that Cd was mainly stored in cell walls, which also explains the reason for chlorophyll content and photosynthesis index observing no significant changes (Figs. S10 and 11). Cd affects the cellular processes occurring in the chloroplasts and mitochondria to varied extent (Mwamba et al., 2016). After penetrating the leaves, Cd is mainly transported to other plant tissues in the form of complexes via the phloem vascular system, similar to photosynthates (Page and Feller, 2015; Clemens and Ma, 2016). Certain metal-binding compounds, including nicotianamine and phytochelatins, are considered to be involved in heavy metal transport in the phloem (Mendoza-Cózatl et al., 2008; Hazama et al., 2015); phytochelatins and glutathione can function as long-distance carriers of Cd in the phloem (Mendoza-Cózatl et al., 2008). Cd is redistributed within the shoots via the phloem and is delivered to the roots, newly formed leaves, and wheat grains (Cakmak et al., 2000a, 2000b; Page and Feller, 2005; Page et al., 2006). However, how Cd is loaded into the phloem, transported via the phloem, and ultimate transferred into the grain is unclear (Clemens and Ma, 2016). In this study, the CdS_N penetrating the leaf surface, was transferred to the stems and roots, which may elevate the Cd concentration in vegetables;thus, Cd accumulation in humans may increase by consuming vegetables from such affected areas. Furthermore, the cell wall, which is mainly composed of cellulose and matrix polysaccharides (pectins and hemicelluloses), is a source of dietary fiber (Cosgrove, 2005; Dhingra et al., 2012); excess accumulation of Cd in cell walls may therefore elevate the risk of toxic Cd entering the food chain.

Before consuming the vegetable, the leaves were carefully washed to remove deposited surface contaminants. However, this washing process may not have been sufficient to remove internalized contaminants (Kozlov et al., 2000; Hong et al., 2014). Contaminants may still have been present on the cuticle, leaf epidermis, and the epicuticular waxes of leaves (Eichert et al., 2008; Larue et al., 2014a, 2014b; Schreck et al., 2014), signifying the necessity of assessing the human health risks associated with consuming such vegetables. Compared with the EDI and MDI values of the exposed WS and PC, the EDI values of the CK were all below the tolerable daily intake limit (TDI, 1.0 μg kg^{-1} day^{-1}) at 0.07

and 0.09 μg kg^{-1} day^{-1}, respectively. However, the EDI values of the higher concentration treatments (25 and 125 mg L^{-1} for WS, and 125 mg L^{-1} for PC) ranged from 2.35 to 8.61 μg kg^{-1} day^{-1}, which are 2.35–8.61 times that of the TDI (Table S6). In addition, the HQ values of the higher concentration treatments (25 and 125 mg L^{-1} for WS, and 125 mg L^{-1} for PC) were above one (> 1) and are 28, 103, and 38 times higher than those in CK, respectively (Table S6), suggesting that the consumption of these vegetables would pose a serious health hazard. This is consistent with previous reports in which the long-term exposure of vegetables to metal nanoparticles was found to increase metal nanoparticle accumulation in vegetables, threatening human health via the food chain (Xiong et al., 2017; Liu et al., 2019). Moreover, the MDI values for higher concentration treatments (25 and 125 mg L^{-1}) ranged from 1.91 to 19.8 g DW day^{-1}. Such quantities could easily be present in vegetables consumed by adults. Thus, the impact of foliar exposure should be considered in Cd-related health risk assessments of edible vegetables.

4. Conclusion

The current study shows that WS and PC can absorb CdS_N via foliar exposure. Stomatal openings were likely the main Cd uptake pathway in the leaves of both species.The growth and Cd accumulation of plants demonstrated no obvious differences between CdS_N and the corresponding CdS_B. The Cd may be translocated from the leaves to other plant tissues, resulting in a significantly increase in their concentration. Exposure concentration, rather than particle size and solubility, regulated the foliar uptake and storage of Cd. Subcellular analysis and NanoSIMS images show that Cd was distributed in the soluble fraction and cell walls of the leaves, which may be an effective Cd detoxification mechanism. Due to plant detoxification no evident phytotoxicity was observed. However, a higher health risk resulting from consuming vegetables exposed to foliar Cd is likely to exist. This study provides information regarding foliar CdS_N and CdS_B uptake, accumulation, and distribution in WS and PC, which will aid in reducing the risks associated with atmospheric Cd, ensuring food safety and security. Metals underwent changes in speciation after foliar uptake and affected their biochemical behavior inside plants. Thus, further soil pot experiments should be conducted to determine the localization and speciation of Cd in plants.

CRediT authorship contribution statement

Xiaoxue Ouyang: Investigation, Methodology, Data analysis, Writing – original draft. **Jie Ma:** Conceptualization, Writing – review & editing, Funding acquisition. **Ran Zhang:** Investigation. **Pan Li:** Writing – review & editing. **Man Gao:** Resources. **Yali Chen:** Resources. **Chuanqiang Sun:** Resources. **Liping Weng:** Supervision, Conceptualization, Methodology, Writing – review & editing, Funding acquisition. **Sun Yan:** Funding acquisition. **Yongtao Li:** Supervision, Resources.

Declaration of Competing Interest

The authors declare that they have no known competing financial interests or personal relationships that could have appeared to influence the work reported in this paper.

Acknowledgments

The study is financially supported by the National Natural Science Foundation of China (No. 41701262 and 41807143) and Central Public-interest Scientific Institution Basal Research Fund of China (Y2020PT03).

Appendix A. Supporting information

Supplementary data associated with this article can be found in the online version at doi:10.1016/j.jhazmat.2022.128624.

References

Bernal, M., Cases, R., Picorel, R., Yruela, I., 2007. Foliar and root Cu supply affect differently Fe- and Zn-uptake and photosynthetic activity in soybean plants. Environ. Exp. Bot. 60 (2), 145–150. https://doi.org/10.1016/j.envexpbot.2006.09.005.

Bu, Y., Chen, Z., Li, W., Yu, J., 2013. High-efficiency photoelectrochemical properties by a highly crystalline CdS-sensitized ZnO nanorod array. ACS Appl. Mater. Interfaces 5 (11), 5097–5104. https://doi.org/10.1021/am400964c.

Cakmak, I., R.M, W., Hart, J., W.A, N., Oztürk, L., L.V, K., 2000a. Uptake and retranslocation of leaf-applied cadmium (109Cd) in diploid, tetraploid and hexaploid wheats. J. Exp. Bot. (343), 343. https://doi.org/10.1093/jexbot/51.343.221.

Cakmak, I., Welch, R.M., Erenoglu, B., Römheld, V., Norvell, W.A., Kochian, L.V., 2000b. Influence of varied zinc supply on re-translocation of cadmium (109Cd) and rubidium (86Rb) applied on mature leaf of durum wheat seedlings. Plant Soil 219 (1), 279–284. https://doi.org/10.1023/A:1004777631452.

Canepari, S., Perrino, C., Olivieri, F., Astolfi, M.L., 2008. Characterisation of the traffic sources of PM through size-segregated sampling, sequential leaching and ICP analysis. Atmos. Environ. 42 (35), 8161–8175. https://doi.org/10.1016/j.atmosenv.2008.07.052.

Cao, X.Y., Tan, C.Y., Wu, L.H., Luo, Y.M., He, Q.H., Liang, Y.F., Peng, B., Christie, P., 2020. Atmospheric deposition of cadmium in an urbanized region and the effect of simulated wet precipitation on the uptake performance of rice. Sci. Total Environ. 700, 134513 https://doi.org/10.1016/j.scitotenv.2019.134513.

Chang, Y.S., Chang, Y.J., Lin, C.T., Lee, M.C., Wu, C.W., Lai, Y.H., 2013. Nitrogen fertilization promotes the phytoremediation of cadmium in Pentas lanceolata. Int. Biodeterior. Biodegrad. 85, 709–714. https://doi.org/10.1016/j.ibiod.2013.05.021.

Clemens, S., Ma, J.F., 2016. Toxic heavy metal and metalloid accumulation in crop plants and foods. Annu. Rev. Plant Biol. 67, 489–512. https://doi.org/10.1146/annurev-arplant-043015-112301.

Cosgrove, D.J., 2005. Growth of the plant cell wall. Nat. Rev. Mol. Cell Biol. 6 (11), 850–861. https://doi.org/10.1038/nrm1746.

De Temmerman, L., Ruttens, A., Waegeneers, N., 2012. Impact of atmospheric deposition of As, Cd and Pb on their concentration in carrot and celeriac. Environ. Pollut. 166, 187–195. https://doi.org/10.1016/j.envpol.2012.03.032.

Dhingra, D., Michael, M., Rajput, H., Patil, R.T., 2012. Dietary fibre in foods: a review. J. Food Sci. Technol. 49 (3), 255–266. https://doi.org/10.1007/s13197-011-0365-5.

Dietz, K.J., Herth, S., 2011. Plant nanotoxicology. Trends Plant Sci. 16 (11), 582–589. https://doi.org/10.1016/j.tplants.2011.08.003.

Dillner, A.M., Schauer, J.J., Christensen, W.F., Cass, G.R., 2005. A quantitative method for clustering size distributions of elements. Atmos. Environ. 39 (8), 1525–1537. https://doi.org/10.1016/j.atmosenv.2004.11.035.

Eichert, T., Goldbach, H.E., 2008. Equivalent pore radii of hydrophilic foliar uptake routes in stomatous and astomatous leaf surfaces–further evidence for a stomatal pathway. Physiol. Plant. 132 (4), 491–502. https://doi.org/10.1111/j.1399-3054.2007.01023.x.

Eichert, T., Kurtz, A., Steiner, U., Goldbach, H.E., 2008. Size exclusion limits and lateral heterogeneity of the stomatal foliar uptake pathway for aqueous solutes and water-suspended nanoparticles. Physiol. Plant 134 (1), 151–160. https://doi.org/10.1111/j.1399-3054.2008.01135.x.

Feng, W.L., Guo, Z.H., Xiao, X.Y., Peng, C.H., Shi, L., Ran, H.Z., Xu, W.X., 2019. Atmospheric deposition as a source of cadmium and lead to soil-rice system and associated risk assessment. Ecotoxicol. Environ. Saf. 180, 160–167. https://doi.org/10.1016/j.ecoenv.2019.04.090.

Fernández, V., Eichert, T., 2009. Uptake of hydrophilic solutes through plant leaves: current state of knowledge and perspectives of foliar fertilization. Crit. Rev. Plant Sci. 28 (1–2), 36–68. https://doi.org/10.1080/07352680902743069.

Fernandez-Olmo, I., Puente, M., Montecalvo, L., Irabien, A., 2014. Source contribution to the bulk atmospheric deposition of minor and trace elements in a Northern Spanish coastal urban area. Atmos. Res 145, 80–91. https://doi.org/10.1016/j.atmosres.2014.04.002.

Fu, Q., Lai, J.L., Tao, Z.Y., Han, N., Wu, G., 2016. Characterizations of bio-accumulations, subcellular distribution and chemical forms of cesium in Brassica juncea, and Vicia faba. J. Environ. Radio. 154, 52–59. https://doi.org/10.1016/j.jenvrad.2016.01.016.

Fu, X., Dou, C., Chen, Y., Chen, X., Shi, J., Yu, M., Xu, J., 2011. Subcellular distribution and chemical forms of cadmium in Phytolacca americana L. J. Hazard. Mater. 186 (1), 103–107. https://doi.org/10.1016/j.jhazmat.2010.10.122.

Gao, P.P., Xue, P.Y., Dong, J.W., Zhang, X.M., Sun, H.X., Geng, L.P., Luo, S.X., Zhao, J.J., Liu, W.J., 2021. Contribution of PM2.5-Pb in atmospheric fallout to Pb accumulation in Chinese cabbage leaves via stomata. J. Hazard. Mater. 407, 124356 https://doi.org/10.1016/j.jhazmat.2020.124356.

Hao, X., Li, T., Yu, H., Zhang, X., Zheng, Z., Chen, G., Zhang, S., Zhao, L., Pu, Y., 2015. Cd accumulation and subcellular distribution in two ecotypes of Kyllinga brevifolia Rottb as affected by Cd treatments. Environ. Sci. Pollut. Res. 22 (10), 7461–7469. https://doi.org/10.1007/s11356-015-4379-9.

Harris, N.S., Taylor, G.J., 2001. Remobilization of cadmium in maturing shoots of near isogenic lines of durum wheat that differ in grain cadmium accumulation. J. Exp. Bot. 52 (360), 1473–1481. https://doi.org/10.1093/jexbot/52.360.1473.

Hassanien, M.A., Shahawy, A.M.E., 2011. Environmental heavy metals and mental disorders of children in developing countries. In: Simeonov, L.I., Kochubovski, M.V., Simeonova, B.G. (Eds.), Environmental Heavy Metal Pollution and Effects on Child Mental Development. Springer Netherlands, Dordrecht, pp. 1–25.

Hazama, K., Nagata, S., Fujimori, T., Yanagisawa, S., Yoneyama, T., 2015. Concentrations of metals and potential metal-binding compounds and speciation of Cd, Zn and Cu in phloem and xylem saps from castor bean plants (Ricinus communis) treated with four levels of cadmium. Physiol. Plant. 154 (2), 243–255. https://doi.org/10.1111/ppl.12309.

Hong, J., Peralta-Videa, J.R., Rico, C., Sahi, S., Viveros, M.N., Bartonjo, J., Zhao, L., Gardea-Torresdey, J.L., 2014. Evidence of translocation and physiological impacts of foliar applied CeO2 nanoparticles on cucumber (Cucumis sativus) plants. Environ. Sci. Technol. 48 (8), 4376–4385. https://doi.org/10.1021/es404931g.

Kilburn, M.R., Clode, P.L., 2014. Elemental and Isotopic Imaging of Biological Samples Using NanoSIMS. In: Kuo, J. (Ed.), Electron Microscopy: Methods and Protocols. Humana Press, Totowa, NJ, pp. 733–755.

Kozlov, M.V., Haukioja, E., Bakhtiarov, A.V., Stroganov, D.N., Zimina, S.N., 2000. Root versus canopy uptake of heavy metals by birch in an industrially polluted area: contrasting behaviour of nickel and copper. Environ. Pollut. 107 (3), 413–420. https://doi.org/10.1016/S0269-7491(99)00159-1.

Kubier, A., Wilkin, R.T., Pichler, T., 2019. Cadmium in soils and groundwater: a review. Appl. Geochem. 108, 1–16. https://doi.org/10.1016/j.apgeochem.2019.104388.

Kuloglu, E., Tuncel, G., 2005. Size distribution of trace elements and major ions in the eastern Mediterranean atmosphere. Water Air Soil Pollut. 167 (1–4), 221–241. https://doi.org/10.1007/s11270-005-8651-3.

Kumar, S., Prasad, S., Yadav, K.K., 2019. Utilization of air pollutants by plants: need for present and future scrutiny. J. Agric. Food Chem. 67 (10), 2741–2742. https://doi.org/10.1021/acs.jafc.9b00921.

Larue, C., Castillo-Michel, H., Sobanska, S., Cécillon, L., Bureau, S., Barthès, V., Ouerdane, L., Carrière, M., Sarret, G., 2014a. Foliar exposure of the crop Lactuca sativa to silver nanoparticles: evidence for internalization and changes in Ag speciation. J. Hazard. Mater. 264, 98–106. https://doi.org/10.1016/j.jhazmat.2013.10.053.

Larue, C., Castillo-Michel, H., Sobanska, S., Trcera, N., Sorieul, S., Cécillon, L., Ouerdane, L., Legros, S., Sarret, G., 2014b. Fate of pristine TiO2 nanoparticles and aged paint-containing TiO2 nanoparticles in lettuce crop after foliar exposure. J. Hazard. Mater. 273, 17–26. https://doi.org/10.1016/j.jhazmat.2014.03.014.

Lead, J.R., Wilkinson, K.J., Environmental Colloids and Particles: Current Knowledge and Future Developments, in: Environmental Colloids and Particles, 2006b, pp. 1–15.

Lead, J.R., Wilkinson, K.J., 2006a. Aquatic colloids and nanoparticles: current knowledge and future trends. Environ. Chem. 3 (3) https://doi.org/10.1071/en06025.

Lee, P.-K., Choi, B.-Y., Kang, M.-J., 2015. Assessment of mobility and bio-availability of heavy metals in dry depositions of Asian dust and implications for environmental risk. Chemosphere 119, 1411–1421. https://doi.org/10.1016/j.chemosphere.2014.10.028.

Li, L.P., Zhang, Y.Q., Ippolito, J.A., Xing, W.Q., Qiu, K.Y., Wang, Y.L., 2020a. Cadmium foliar application affects wheat Cd, Cu, Pb and Zn accumulation. Environ. Pollut. 262, 114329 https://doi.org/10.1016/j.envpol.2020.114329.

Li, W.Q., Qing, T., Li, C.C., Li, F., Ge, F., Fei, J.J., Peijnenburg, W.J.G.M., 2020b. Integration of subcellular partitioning and chemical forms to understand silver nanoparticles toxicity to lettuce (Lactuca sativa L.) under different exposure pathways. Chemosphere. https://doi.org/10.1016/j.chemosphere.2020.127349.

Liu, H.L., Zhou, J., Li, M., Hu, Y.M., Liu, X., Zhou, J., 2019. Study of the bioavailability of heavy metals from atmospheric deposition on the soil-pakchoi (Brassica chinensis L.) system. J. Hazard. Mater. 362, 9–16. https://doi.org/10.1016/j.jhazmat.2018.09.032.

Lopez-Millan, A.F., Sagardoy, R., Solanas, M., Abadia, A., Abadia, J., 2009. Cadmium toxicity in tomato (Lycopersicon esculentum) plants grown in hydroponics. Environ. Exp. Bot. 65 (2–3), 376–385. https://doi.org/10.1016/j.envexpbot.2008.11.010.

Louie, P., Watson, J., Chow, J., Chen, A., Sin, D., Lau, A., 2005. Seasonal characteristics and regional transport of PM in Hong Kong. Atmos. Environ. 39, 1695–1710. https://doi.org/10.1016/j.atmosenv.2004.11.017.

Luo, L., Ma, Y., Zhang, S., Wei, D., Zhu, Y.-G., 2009. An inventory of trace element inputs to agricultural soils in China. J. Environ. Manag. 90 (8), 2524–2530. https://doi.org/10.1016/j.jenvman.2009.01.011.

Mendoza-Cózatl, D.G., Butko, E., Springer, F., Torpey, J.W., Komives, E.A., Kehr, J., Schroeder, J.I., 2008. Identification of high levels of phytochelatins, glutathione and cadmium in the phloem sap of Brassica napus. A role for thiol-peptides in the long-distance transport of cadmium and the effect of cadmium on iron translocation. Plant J. 54 (2), 249–259. https://doi.org/10.1111/j.1365-313X.2008.03410.x.

Mugford, S.G., Lee, B.R., Koprivova, A., Matthewman, C., Kopriva, S., 2011. Control of sulfur partitioning between primary and secondary metabolism. Plant J. 65 (1), 96–105. https://doi.org/10.1111/j.1365-313X.2010.04410.x.

Mwamba, T.M., Li, L., Gill, R.A., Islam, F., Nawaz, A., Ali, B., Farooq, M.A., Lwalaba, J.L., Zhou, W.J., 2016. Differential subcellular distribution and chemical forms of cadmium and copper in Brassica napus. Ecotoxicol. Environ. Saf. 134, 239–249. https://doi.org/10.1016/j.ecoenv.2016.08.021.

Ondrasek, G., Clode, P.L., Kilburn, M.R., Guagliardo, P., Romic, D., Rengel, Z., 2019. Zinc and cadmium mapping in the apical shoot and hypocotyl tissues of radish by high-resolution secondary ion mass spectrometry (NanoSIMS) after short-term exposure to metal contamination. Int. J. Env. Res. Public Health 16 (3). https://doi.org/10.3390/ijerph16030373.

Page, V., Feller, U., 2005. Selective transport of zinc, manganese, nickel, cobalt and cadmium in the root system and transfer to the leaves in young wheat plants. Ann. Bot. 96 (3), 425–434. https://doi.org/10.1093/aob/mci189.

Page, V., Feller, U., 2015. Heavy metals in crop plants: transport and redistribution processes on the whole plant level. Agronomy 5 (3), 447–463. https://doi.org/10.3390/agronomy5030447.

Page, V., Weisskopf, L., Feller, U., 2006. Heavy metals in white lupin: uptake, root-to-shoot transfer and redistribution within the plant. N. Phytol. 171 (2), 329–341. https://doi.org/10.1111/j.1469-8137.2006.01756.x.

Pan, Y., Wang, Y., 2015. Atmospheric wet and dry deposition of trace elements at ten sites in Northern China. Atmos. Chem. Phys. Discuss. 14. https://doi.org/10.5194/acpd-14-20647-2014.

Pittman, J.K., 2005. Managing the manganese: molecular mechanisms of manganese transport and homeostasis. N. Phytol. 167 (3), 733–742. https://doi.org/10.1111/j.1469-8137.2005.01453.x.

Pontevedra-Pombal, X., Mighall, T.M., Nóvoa-Muñoz, J.C., Peiteado-Varela, E., Rodríguez-Racedo, J., García-Rodeja, E., Martínez-Cortizas, A., 2013. Five thousand years of atmospheric Ni, Zn, As, and Cd deposition recorded in bogs from NW Iberia: prehistoric and historic anthropogenic contributions. J. Archaeol. Sci. 40 (1), 764–777. https://doi.org/10.1016/j.jas.2012.07.010.

Qaswar, M., Hussain, S., Rengel, Z., 2017. Zinc fertilisation increases grain zinc and reduces grain lead and cadmium concentrations more in zinc-biofortified than standard wheat cultivar. Sci. Total Environ. 605–606, 454–460. https://doi.org/10.1016/j.scitotenv.2017.06.242.

Ramos, I., Esteban, E., Lucena, J.J., Gárate, An, 2002. Cadmium uptake and subcellular distribution in plants of Lactuca sp. Cd /Mn interaction. Plant Sci. 162, 761–767. https://doi.org/10.1016/S0168-9452(02)00017-1.

Riesen, O., Feller, U., 2005. Redistribution of nickel, cobalt, manganese, zinc, and cadmium via the phloem in young and maturing wheat. J. Plant Nutr. 28 (3), 421–430. https://doi.org/10.1081/pln-200049153.

Rizwan, M., Ali, S., Abbas, T., Zia-ur-Rehman, M., Hannan, F., Keller, C., Al-Wabel, M.I., Ok, Y.S., 2016a. Cadmium minimization in wheat: A critical review. Ecotoxicol. Environ. Saf. 130, 43–53. https://doi.org/10.1016/j.ecoenv.2016.04.001.

Rizwan, M., Ali, S., Adrees, M., Rizvi, H., Zia-Ur-Rehman, M., Hannan, F., Qayyum, M.F., Hafeez, F., Ok, Y.S., 2016b. Cadmium stress in rice: toxic effects, tolerance mechanisms, and management: a critical review. Environ. Sci. Pollut. Res. 23 (18), 17859–17879. https://doi.org/10.1007/s11356-016-6436-4.

Rizwan, M., Ali, S., Adrees, M., Ibrahim, M., Tsang, D.C.W., Zia-ur-Rehman, M., Zahir, Z. A., Rinklebe, J., Tack, F.M.G., Ok, Y.S., 2017. A critical review on effects, tolerance mechanisms and management of cadmium in vegetables. Chemosphere 182, 90–105. https://doi.org/10.1016/j.chemosphere.2017.05.013.

Rodriguez-Rosales, M.P., Jiang, X., Galvez, F.J., Aranda, M.N., Cubero, B., Venema, K., 2008. Overexpression of the tomato K+/H+ antiporter LeNHX2 confers salt tolerance by improving potassium compartmentalization. N. Phytol. 179 (2), 366–377. https://doi.org/10.1111/j.1469-8137.2008.02461.x.

Rodriguez-Serrano, M., Romero-Puertas, M.C., Pazmino, D.M., Testillano, P.S., Risueno, M.C., Del Rio, L.A., Sandalio, L.M., 2009. Cellular response of pea plants to cadmium toxicity: cross talk between reactive oxygen species, nitric oxide, and calcium. Plant J. 150 (1), 229–243. https://doi.org/10.1104/pp.108.131524.

Schonherr, J., 2006. Characterization of aqueous pores in plant cuticles and permeation of ionic solutes. J. Exp. Bot. 57 (11), 2471–2491. https://doi.org/10.1093/jxb/erj217.

Schönherr, J., Luber, M., 2001. Cuticular penetration of potassium salts: effects of humidity, anions, and temperature. Plant Soil 236 (1), 117–122. https://doi.org/10.1023/A:1011976727078.

Schreck, E., Foucault, Y., Sarret, G., Sobanska, S., Cécillon, L., Castrec-Rouelle, M., Uzu, G., Dumat, C., 2012. Metal and metalloid foliar uptake by various plant species exposed to atmospheric industrial fallout: mechanisms involved for lead. Sci. Total Environ. 427–428, 253–262. https://doi.org/10.1016/j.scitotenv.2012.03.051.

Schreck, E., Dappe, V., Sarret, G., Sobanska, S., Nowak, D., Nowak, J., Stefaniak, E.A., Magnin, V., Ranieri, V., Dumat, C., 2014. Foliar or root exposures to smelter particles: consequences for lead compartmentalization and speciation in plant leaves. Sci. Total Environ. 476–477, 667–676. https://doi.org/10.1016/j.scitotenv.2013.12.089.

Schreiber, L., Önherr, J., 2009. Water and Solute Permeability of Plant Cuticles: Measurement and Data Analysis. Water and Solute Permeability of Plant Cuticles: Measurement and Data Analysis. 1–299. http://doi.org/10.1007/978-3-540-68945-4.

Shahid, M., Dumat, C., Khalid, S., Schreck, E., Xiong, T.T., Niazi, N.K., 2017. Foliar heavy metal uptake, toxicity and detoxification in plants: a comparison of foliar and root metal uptake. J. Hazard. Mater. 325, 36–58. https://doi.org/10.1016/j.jhazmat.2016.11.063.

Shao, X., Cheng, H.G., Li, Q., Lin, C.Y., 2013. Anthropogenic atmospheric emissions of cadmium in China. Atmos. Environ. 79, 155–160. https://doi.org/10.1016/j.atmosenv.2013.05.055.

Shi, G.L., Li, D.J., Wang, Y.F., Liu, C.H., Hu, Z.B., Lou, L.Q., Rengel, Z., Cai, Q.S., 2019. Accumulation and distribution of arsenic and cadmium in winter wheat (Triticum aestivum L.) at different developmental stages. Sci. Total Environ. 667, 532–539. https://doi.org/10.1016/j.scitotenv.2019.02.394.

Smart, K.E., Kilburn, M.R., Salter, C.J., Smith, J.A.C., Grovenor, C.R.M., 2007. NanoSIMS and EPMA analysis of nickel localisation in leaves of the hyperaccumulator plant Alyssum lesbiacum. Int. J. Mass Spectrom. 260 (2–3), 107–114. https://doi.org/10.1016/j.ijms.2006.08.011.

Smart, K.E., Smith, J.A., Kilburn, M.R., Martin, B.G., Hawes, C., Grovenor, C.R., 2010. High-resolution elemental localization in vacuolate plant cells by nanoscale

secondary ion mass spectrometry. Plant J. 63 (5), 870–879. https://doi.org/10.1111/j.1365-313X.2010.04279.x.
Tartivel, R., Tatin, R., Delhaye, T., Maupas, A., Gendron, A., Gautier, S., Lavastre, O., 2012. Visualization and localization of bromotoluene distribution in Hedera helix using NanoSIMS. Chemosphere 89 (7), 805–809. https://doi.org/10.1016/j.chemosphere.2012.04.058.
Tavarez, M., Macri, A., Sankaran, R.P., 2015. Cadmium and zinc partitioning and accumulation during grain filling in two near isogenic lines of durum wheat. Plant Physiol. Biochem. 97, 461–469. https://doi.org/10.1016/j.plaphy.2015.10.024.
Uzu, G., Sobanska, S., Sarret, G., Muñoz, M., Dumat, C., 2010. Foliar lead uptake by lettuce exposed to atmospheric fallouts. Environ. Sci. Technol. 44 (3), 1036–1042. https://doi.org/10.1021/es902190u.
Uzu, G., Sauvain, J.J., Baeza-Squiban, A., Riediker, M., Hohl, M.S., Val, S., Tack, K., Denys, S., Pradere, P., Dumat, C., 2011. In vitro assessment of the pulmonary toxicity and gastric availability of lead-rich particles from a lead recycling plant. Environ. Sci. Technol. 45 (18), 7888–7895. https://doi.org/10.1021/es200374c.
Vecerova, K., Vecera, Z., Docekal, B., Oravec, M., Pompeiano, A., Triska, J., Urban, O., 2016. Changes of primary and secondary metabolites in barley plants exposed to CdO nanoparticles. Environ. Pollut. 218, 207–218. https://doi.org/10.1016/j.envpol.2016.05.013.
Vecerova, K., Vecera, Z., Mikuska, P., Coufalik, P., Oravec, M., Docekal, B., Novotna, K., Vesela, B., Pompeiano, A., Urban, O., 2019. Temperature alters susceptibility of Picea abies seedlings to airborne pollutants: the case of CdO nanoparticles. Environ. Pollut. 253, 646–654. https://doi.org/10.1016/j.envpol.2019.07.061.
Verma, P., George, K.V., Singh, H.V., Singh, R.N., 2007. Modeling cadmium accumulation in radish, carrot, spinach and cabbage. Appl. Math. Model. 31 (8), 1652–1661. https://doi.org/10.1016/j.apm.2006.05.008.
Wang, J., Zhao, W.W., Tian, C.Y., Xu, J.J., Chen, H.Y., 2012. Highly efficient quenching of electrochemiluminescence from CdS nanocrystal film based on biocatalytic deposition. Talanta 89, 422–426. https://doi.org/10.1016/j.talanta.2011.12.055.
Wang, J.B., Su, L.Y., Yang, J.Z., Yuan, J.G., Yin, A.G., Qiu, Q., Zhang, K., Yang, Z.Y., 2015. Comparisons of cadmium subcellular distribution and chemical forms between low-Cd and high-Cd accumulation genotypes of watercress (Nasturtium officinale L. R. Br.). Plant Soil 396 (1–2), 325–337. https://doi.org/10.1007/s11104-015-2580-8.
Wang, X., Liu, Y.G., Zeng, G.M., Chai, L.Y., Song, X.C., Min, Z.Y., Xiao, X., 2008. Subcellular distribution and chemical forms of cadmium in Bechmeria nivea (L.) Gaud. Environ. Exp. Bot. 62 (3), 389–395. https://doi.org/10.1016/j.envexpbot.2007.10.014.
White, P.J., Brown, P.H., 2010. Plant nutrition for sustainable development and global health. Ann. Bot. 105 (7), 1073–1080. https://doi.org/10.1093/aob/mcq085.
Worms, I., Simon, D.F., Hassler, C.S., Wilkinson, K.J., 2006. Bioavailability of trace metals to aquatic microorganisms: importance of chemical, biological and physical processes on biouptake. Biochimie 88 (11), 1721–1731. https://doi.org/10.1016/j.biochi.2006.09.008.
Wu, F.B., Dong, J., Qian, Q.Q., Zhang, G.P., 2005. Subcellular distribution and chemical form of Cd and Cd-Zn interaction in different barley genotypes. Chemosphere 60 (10), 1437–1446. https://doi.org/10.1016/j.chemosphere.2005.01.071.
Wu, L., Zhou, J., Zhou, T., Li, Z., Jiang, J., Zhu, D., Hou, J., Wang, Z., Luo, Y., Christie, P., 2018. Estimating cadmium availability to the hyperaccumulator Sedum plumbizincicola in a wide range of soil types using a piecewise function. Sci. Total Environ. 637–638, 1342–1350. https://doi.org/10.1016/j.scitotenv.2018.04.386.
Xin, J., Huang, B., 2014. Subcellular distribution and chemical forms of cadmium in two hot pepper cultivars differing in cadmium accumulation. J. Agric. Food Chem. 62 (2), 508–515. https://doi.org/10.1021/jf4044524.
Xiong, T.T., Leveque, T., Shahid, M., Foucault, Y., Mombo, S., Dumat, C., 2014. Lead and cadmium phytoavailability and human bioaccessibility for vegetables exposed to soil or atmospheric pollution by process ultrafine particles. J. Environ. Qual. 43 (5) https://doi.org/10.2134/jeq2013.11.0469.
Xiong, T.T., Dumat, C., Dappe, V., Vezin, H., Schreck, E., Shahid, M., Pierart, A., Sobanska, S., 2017. Copper oxide nanoparticle foliar uptake, phytotoxicity, and consequences for sustainable urban agriculture. Environ. Sci. Technol. 51 (9), 5242–5251. https://doi.org/10.1021/acs.est.6b05546.
Xu, Q., Min, H., Cai, S., Fu, Y., Sha, S., Xie, K., Du, K., 2012. Subcellular distribution and toxicity of cadmium in Potamogeton crispus L. Chemosphere 89 (1), 114–120. https://doi.org/10.1016/j.chemosphere.2012.04.046.
Yang, J.X., Guo, H.T., Ma, Y.B., Wang, L.Q., Wei, D.P., Hua, L., 2010. Genotypic variations in the accumulation of Cd exhibited by different vegetables. J. Environ. Sci. (China). 22 (8), 1246–1252. https://doi.org/10.1016/s1001-0742(09)60245-x.
Yang, Y., Zhang, F.S., Li, H.F., Jiang, R.F., 2009. Accumulation of cadmium in the edible parts of six vegetable species grown in Cd-contaminated soils. J. Environ. Manag. 90 (2), 1117–1122. https://doi.org/10.1016/j.jenvman.2008.05.004.
Zereini, F., Alt, F., Messerschmidt, J., Wiseman, C., Feldmann, I., von Bohlen, A., Müller, J., Liebl, K., Püttmann, W., 2005. Concentration and Distribution of Heavy Metals in Urban Airborne Particulate Matter in Frankfurt am Main, Germany. Environ. Sci. Technol. 39 (9), 2983–2989. https://doi.org/10.1021/es040040t.
Zhang, H., Guo, Q., Yang, J., Shen, J., Chen, T., Zhu, G., Chen, H., Shao, C., 2015. Subcellular cadmium distribution and antioxidant enzymatic activities in the leaves of two castor (Ricinus communis L.) cultivars exhibit differences in Cd accumulation. Ecotoxicol. Environ. Saf. 120, 184–192. https://doi.org/10.1016/j.ecoenv.2015.06.003.
Zhou, J., Wan, H., He, J., Lyu, D., Li, H., 2017. Integration of cadmium accumulation, subcellular distribution, and physiological responses to understand cadmium tolerance in apple rootstocks. Front. Plant Sci. 8, 966. https://doi.org/10.3389/fpls.2017.00966.
Zhu, Q.H., Huang, D.Y., Liu, S.L., Luo, Z.C., Rao, Z.X., Cao, X.L., Ren, X.F., 2013. Accumulation and subcellular distribution of cadmiumin ramie (Boehmeria nivea L. Gaud.) planted on elevated soil cadmium contents. Plant Soil Environ. 59 (2), 57–61. https://doi.org/10.17221/439/2012-PSE.
Zornoza, P., Vázquez, S., Esteban, E., Fernández-Pascual, M., Carpena, R., 2002. Cadmium-stress in nodulated white lupin: strategies to avoid toxicity. Plant Physiol. Biochem. 40 (12), 1003–1009. https://doi.org/10.1016/S0981-9428(02)01464-X.